

Structural evolution of protein-biofilms: Simulations and Experiments

Y. Schmitt, H. Hähl, C. Gilow, H. Mantz and K. Jacobs

Department of Experimental Physics, Saarland University, 66041 Saarbrücken, Germany

O. Leidinger, M. Bellion and L. Santen

Department of Theoretical Physics, Saarland University, 66041 Saarbrücken, Germany

(Dated: November 9, 2021)

The control of biofilm formation is a challenging goal that has not been reached yet in many aspects. One is the role of van der Waals forces and another the importance of mutual interactions between the adsorbing and the adsorbed biomolecules ('critical crowding'). Here, a combined experimental and theoretical approach is presented that fundamentally probes both aspects. On three model proteins, lysozyme, α -amylase and bovine serum albumin (BSA), the adsorption kinetics is studied. Composite substrates are used enabling a separation of the short- and the long-range forces. Though usually neglected, experimental evidence is given for the influence of van der Waals forces on the protein adsorption as revealed by *in situ* ellipsometry. The three proteins were chosen for their different conformational stability in order to investigate the influence of conformational changes on the adsorption kinetics. Monte Carlo simulations are used to develop a model for these experimental results by assuming an internal degree of freedom to represent conformational changes. The simulations also provide data on the distribution of adsorption sites. By *in situ* atomic force microscopy we can also test this distribution experimentally which opens the possibility to e.g. investigate the interactions between adsorbed proteins.

Proteins are found to be involved in interactions with solid surfaces in numerous natural events. Due to protein adsorption and subsequent bacterial adherence, biofilms are formed at interfaces between solid substrates and liquids containing biomacromolecules. Biofilm formation as well as protein adsorption are molecular assembly processes occurring at interfaces [1]. Moreover, these processes are collective phenomena, since surface coverage, adsorption kinetics, conformational arrangement etc. are depending on the nature of the molecular neighborhood. The lack of effective control over this process has become a bottleneck impeding the development of many biotechnologies, examples including biosensors, enzyme immobilization in biocatalysis, antibody attachment in immunoassays, biomaterial development, and tissue engineering. During the past decades, substantial progress has been made in understanding some mechanisms of protein adsorption [2–6]. Adsorption is the net result of various types of interactions which depend on the nature of the protein and of the substrate, as well as on the surrounding aqueous solution. Several driving forces have been identified for the protein adsorption process, including dehydration of the protein and substrate surface, redistribution of charged groups in the interfacial film, and structural rearrangements in the biomolecules. Regarding the role of substrate characteristics, both surface topography and surface chemistry have been shown to affect protein adsorption, bacteria

and cell adhesion [4, 7]. However, since most topographical variations are accompanied by chemical heterogeneities, separating both effects is difficult and a differentiation between the impacts of short- and long-range forces is one step towards gaining control of biofilm formation and has only recently been probed [8, 9]. It is the aim of this paper to compile the results in order to stress that the sub-surface composition is a parameter of utmost importance.

The separation of these short- and long-range interactions is possible using composite samples: By variation of the silicon oxide thickness on top of Si wafers, the van der Waals interactions can be tuned [10–13], as described in section I. The adsorption kinetics of BSA and α -amylase are sensitive to these variations of the long-range potential. Note that the van der Waals interaction depends on the geometry of the interacting objects [14]: For two atoms, the van der Waals potential decreases like $1/r^6$, where r denotes the distance. However, for a spherical particle interacting with a planar surface the decrease is much slower i.e. like $1/r$. Hence, the strength of the van der Waals forces cannot be neglected.

Studies concentrating on the kinetic behavior during adsorption, desorption, and exchange processes revealed that there is a certain hierarchy or intermolecular arrangement of proteins in the adsorption layers (e.g. Schmidt et al. [15]). Additionally, reconfiguration or reorientation of the adsorbed pro-

tein can take place [16, 17]. However, further information is needed to describe the structure of the adsorption layer in detail. A manifold of proteins have actually been detected to undergo conformational changes or reorientations when adsorbed on a variety of hydrophilic, hydrophobic, charged, and uncharged surfaces (e.g. Keselowsky et al. [6], Daly et al. [18], Ishiguro et al. [17], Baujard-Lamotte et al. [19]). These conformational changes and reorientations were interpreted to be a result of mutual interactions between the adsorbed protein molecules (“critical crowding”), as well as interactions between the proteins and between the proteins and the surfaces. Hence, monitoring the conformational change in an adsorbed protein as a function of the adsorption amount and time should be useful for obtaining information about the intermolecular interactions in the adsorption layer.

The direct detection of conformational changes is a challenging task. Most methods are restricted to indirect observations. When monitoring the adsorption kinetics, different kinetic behaviour is found for the ‘rigid’ lysozyme [20] than for α -amylase and BSA [8, 9]. The latter is considered as a ‘soft’ protein [20–23]. This difference in the adsorption kinetics is therefore ascribed to dissimilar tendencies to undergo conformational changes due to adsorption. Monte Carlo simulations including an internal degree of freedom to incorporate conformational changes qualitatively reproduce the experimental findings.

Most methods, like ellipsometry or scattering techniques provide information that is obtained by averaging over some μm^2 . Therefore, these methods cannot provide explicit information about single proteins involved in the adsorption process. A technique that overcomes these shortcomings is atomic force microscopy (AFM). By *in situ* AFM in aqueous environment, the spatial distribution of individual adsorbed proteins can be determined IV and can therefore give new insights into the evolution of protein films. The surface mobility of the single proteins can be tested as well as their tendency to form clusters or to adsorb rather independent from each other, as described in the scenario of random sequential adsorption (RSA) which is presented in section III A.

I. MATERIALS

The proteins α -amylase (product no. 10092), lysozyme (product no. 62971) and bovine serum albumin (product no. A3059) were purchased from Sigma Aldrich, Steinheim, Germany. BSA (66 kDa)[24] and α -amylase (58 kDa)[25] have about the same size but different isoelectric points (pI) at pH 4.7 [26] and 6.5 [25], respectively. For bovine serum albumin (BSA) the ability of showing different conformations is well known [20–23]. Lysozyme has a mass [27] of 14 kDa and its isoelectric point [28] is at pH 11.

As substrates for ellipsometry measurements, silicon surfaces with different silicon dioxide thicknesses were used: natural (2 nm, Wacker Siltronic AG, Burghausen, Germany) and thermally grown (192 nm, Silchem, Freiberg, Germany) dioxide layers, denoted as thin and thick oxide layers in the following. Before usage, the wafers must be cleaned to remove residues from the polishing procedure (mostly hydrocarbons). Therefore, the wafers were immersed into fresh 1:1 $\text{H}_2\text{SO}_4(\text{conc.})/\text{H}_2\text{O}_2(30\%)$ solution for 30 min. Then the acids were removed by rinsing the wafers in hot deionized water, three times 20 min each. All samples were prepared in a clean room environment (class 100), resulting in a water contact angle of 0° directly after cleaning. Nevertheless, upon usage, the silicon wafers showed advancing water contact angles of less than 10° (see Table I for details) and are therefore termed ‘hydrophilic’. To gain a second set of wafers with a ‘hydrophobic’ surface ($\Theta > 90^\circ$), a self-assembled monolayer (SAM) of silane molecules with a CH_3 tailgroup (octadecyltrichlorosilane, OTS, Sigma Aldrich, Germany) was applied to the wafers following standard procedures [29, 30]. The water contact angles on hydrophobized wafers were larger than 110° (Table I) with a hysteresis smaller than 5° . Contact angle hysteresis describes the difference between advancing Θ_a and receding Θ_r contact angles. By additionally measuring the contact angles for glycerol and 1-bromonathalene, the surface energies as well as the Lifshitz-van der Waals and the Lewis acid-base components can be determined [31] as listed in Table II.

Zeta-(ζ)-potential measurements [32] on wafers with thin and thick oxide layers with and without the OTS monolayer were performed for pH values ranging from 2.0 to 7.5 (see Fig. 1). Obviously, the hydrophilic surfaces carry a higher negative charge than the hydrophobic wafers. The oxide layer thickness, however, does not play any role and zeta potential values are identical within the experimental error.

The thicknesses of the silicon oxide and OTS layer were determined by ellipsometry, revealing an oxide thickness of 2 nm for the thin and 192 nm for the thick oxide layers. The thickness of the OTS-SAM is found to be 2.6 nm. The surface roughness of the four wafer types was determined by atomic force microscopy (AFM). The measured root mean square (rms) roughness of an $(1 \mu\text{m})^2$ scan area was below 0.2 nm for all wafer types (see Table I for

TABLE I. Silicon wafer characterization results.

d (SiO) / nm	hydro-	rms / nm	Θ_a^{water}	Θ_r^{water}	$\Theta_a^{glycerol}$	$\Theta_a^{1-bromonaph.}$
2.0(1)	philic	0.09(2)	5(2) $^\circ$	complete wetting	11(3) $^\circ$	13(4) $^\circ$
192(1)	philic	0.13(3)	7(2) $^\circ$	complete wetting	17(3) $^\circ$	15(3) $^\circ$
2.0(1)	phobic	0.12(2)	111(1) $^\circ$	107(1) $^\circ$	95(2) $^\circ$	62(4) $^\circ$
192(1)	phobic	0.15(2)	112(1) $^\circ$	108(2) $^\circ$	92(2) $^\circ$	63(3) $^\circ$

TABLE II. Surface energy γ and their Lifshitz-van der Waals γ^{LW} and Lewis acid-base γ^{AB} components of the substrates, as determined by contact angle measurements, the results of which are listed in Table I.

d (SiO) / nm	hydro-	γ / (mJ/m)	γ^{LW} / (mJ/m)	γ^{AB} / (mJ/m)
2.0(1)	philic	64.2	43.5	20.7
192(1)	philic	63.2	43.1	20.1
2.0(1)	phobic	24.1	24.1	0.0
192(1)	phobic	23.6	23.6	0.0

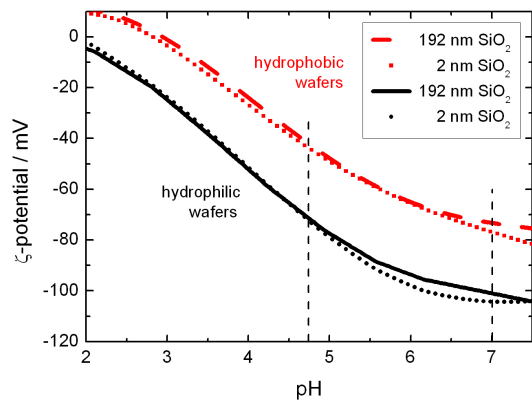


FIG. 1. ζ -potential of hydrophobic and hydrophilic silicon wafers with thin and thick oxide thickness as function of pH. For the ζ -potential, differences in oxide layer thickness are irrelevant. Note that adsorption experiments in this study have been performed at pH 7.0 and 4.75 (vertical dashed lines).

details).

Keeping all other parameters (pH, ionic strength, temperature and protein concentration) constant, the four wafer types allow for the separation of effects due to the long-range and the short-range part of the surface potential [10–13]: Hydrophobization by the OTS-SAM alters the short-range part as can be seen in the contact angle and the ζ -potential. For a substantial alteration of the long-ranged van der Waals potential, the OTS-SAM is too thin. This holds for all molecular-sized layers. The variation of the oxide layer thickness, however, does not have an influence on the short-range potential, since the surface chemistry is identical. Hence contact angle as well as ζ -potential measurements show no difference on thin or thick oxide layers. Vice versa, choosing different subsurface wafer compositions (in our case thin and thick oxide layers) enables an independent variation of

the long-range part, i. e. the van der Waals interaction to probe its influence on the formation of protein films.

The above described four types of Si wafers were used for probing protein film formation by ellipsometry. For the *in situ* AFM experiments shown in the following, mica was chosen as a substrate. Mica is a sheet silicate that can easily be cleaved. When freshly cleaved, mica exhibits an atomically smooth hydrophilic surface. Therefore, mica is frequently used for protein adsorption studies via AFM [33–38].

II. ADSORPTION KINETICS

A. Adsorption studies by ellipsometry

Ellipsometry[39, 40] was used to determine the adsorbed amount of proteins by *in situ* monitoring the adsorption process. The single wavelength ellipsometer (EP³, Nanofilm, Göttingen, Germany) was operated in PCSA (Polarisator-Compensator-Sample-Analyzer) configuration at a wavelength of 532 nm. The ellipsometric angles Ψ and Δ were recorded via the nulling ellipsometry principle with a sampling rate of 1.5 to 6 per minute. This rate was sufficient to monitor the formation of protein layers *in situ*.

To determine the physical properties of the reflecting surface from Ψ and Δ , a model has to be applied [39]. For single wavelength measurements, one has to assume the layers to have a constant height to be able to determine the refractive index and thickness of all layers. For layers with a thickness below 5 nm, it is not possible to distinguish between a change in refractive index and in film thickness [41]. Therefore, de Feijter’s method is applied to determine the adsorbed amount Γ as a function of the refractive index n_f of the protein film with a fixed film thickness d_f

$$\Gamma = d_f \frac{n_f - n_a}{dn/dc} \quad (1)$$

where n_a denotes the refractive index of the ambient and dn/dc the increment of the refractive index of the solution due to the increase of molecule concentration. The refractive index $n(c)$ is assumed to be a linear function[42, 43] with a fixed gradient of $0.183 \text{ cm}^3/\text{g}$.

The measurements were carried out in a temperature controlled closed fluid cell made of Teflon. A connection to a flow system enables a continuous exchange of fluid with constant flow rates and the injection of protein solution via a sample injector (Rheodyne Manual Sample Injector).

The proteins were soluted in a 10 mM phosphate buffer solution (pH 7.0, ionic strength 20 mM). The fluid system was filled with the same buffer and the buffer was run through the fluid cell at a constant flow rate. After reaching a thermal equilibrium (either at 37°C or at room temperature) associated with a constant baseline, the adsorption measurement was started by injecting the protein.

B. Results and discussion

The adsorption kinetics are shown in Fig. 2. They display a typical feature of adsorption kinetics: after a fast initial adsorption, the adsorption rate decreases until a plateau value of adsorbed amount is reached. For lysozyme (Fig. 2 (a)), the decrease of adsorption rate is continuous. This Langmuir-like adsorption kinetics is well described in the literature [2]. The absolute adsorbed amount depends mostly on the chemistry of the surface. The adsorbed amount of lysozyme is higher on hydrophilic samples than on hydrophobic ones. This can be explained by considering the positive net charge[27] of lysozyme ($+8e$) at pH 7 as well as the negative charge of the silicon wafers. The hydrophilic wafers (-103 mV) carry a higher negative charge than the hydrophobic ones (-75 mV), see Fig. 1. Thus, a stronger attractive Coulomb interaction promotes the adsorption on hydrophilic wafers. For lysozyme, we observe no influence of the thickness of the oxide layer on the adsorption kinetics.

For α -amylase (Fig. 2(b)), the adsorption on thick oxide wafers also exhibits a Langmuir-like behavior [8, 9]. On thin silicon oxide, however, the transition between fast initial adsorption and saturation is not continuous. A regime of constant adsorption rate separates the regime of initial adsorption from the saturation. The final adsorbed amount depends only weakly on the oxide thickness but on the hydrophobicity of the surface. In the case of α -amylase, the adsorbed amount is higher on hydrophobic wafers than on hydrophilic ones due to the hydrophobic effect [44]. The higher attraction towards the surface originates from minimizing the contact of water with hydrophobic side groups of the protein and with the hydrophobic surface. As the pH of the solution is close to the isoelectric point of α -amylase (pI 6.9), the protein carries no net charge. Therefore, the Coulomb interac-

tion just plays a minor role for adsorption affinity.

The differences in adsorption behavior between lysozyme and α -amylase are believed to arise from different conformational stabilities [9]. Changes of conformation due to adsorption are frequently described in the literature [20]. As compared to the small and compact lysozyme, α -amylase can be ascribed as a ‘soft’ protein [2]. Therefore, major conformational changes are more likely for α -amylase than for lysozyme.

The third protein in this study, BSA, is known for its ability to change conformation [20–23] e.g. due to changes of the pH of the surrounding solution. As shown in Fig. 3, BSA exhibits a similar adsorption kinetics as α -amylase [9]. On wafers with thin silicon oxide layer (here only experiments on hydrophobic wafers are shown) a regime of constant adsorption rate is observed. When decreasing the temperature from physiological 37°C to room temperature, the regime of constant adsorption rate is elongated. The initial adsorption, however, is only slightly slowed down. Although BSA carries a negative net charge at pH 7 (in contrast to α -amylase), it displays the same two types of adsorption kinetics as α -amylase. Repeating the experiments with acetate buffer at the pI of BSA reveals the same results. Therefore, this effect cannot be explained by charge effects and Coulomb interactions. The appearance of a linear regime must rather depend on the variation of the long-range part of the interaction potential i.e. the van der Waals interaction as well as the conformational stability of the protein.

At this point it has to be stressed that numerous experimental studies focussing on thin film formation or dynamics usually do not give details on the subsurface composition of the samples in the study. The subsurface composition therefore is one to date mostly uncontrolled sample property. It is very likely that many diverse results about biofilm formation of different groups world-wide may be traced back to using different composite samples (still exhibiting the identical surface chemistry). We therefore pledge for a detailed characterization of samples, including e.g. a possible layering. For the widely used Si wafer, for instance, it is inevitable to characterize its oxide layer[45].

Since an experimental study of possible conformational changes of individual proteins during the adsorption process is too challenging to date, colloidal Monte Carlo (MC) simulations were launched using an effective particle model. Here, the sensitivity of the adsorption kinetics to conformational (or even simpler: geometrical) changes of adsorbing objects shall be probed and the results shall then be compared to the experimental findings in order to be able to propose a suitable model. At first sight, a colloidal approach seems too rough to give reliable results for protein adsorption. Yet after checking possible alternatives - which will be done in the following - it shall become clear that - to match the time scale of the experiment, to be able to include conformational changes and to use to date computer power - colloidal MC simulations are the method of choice.

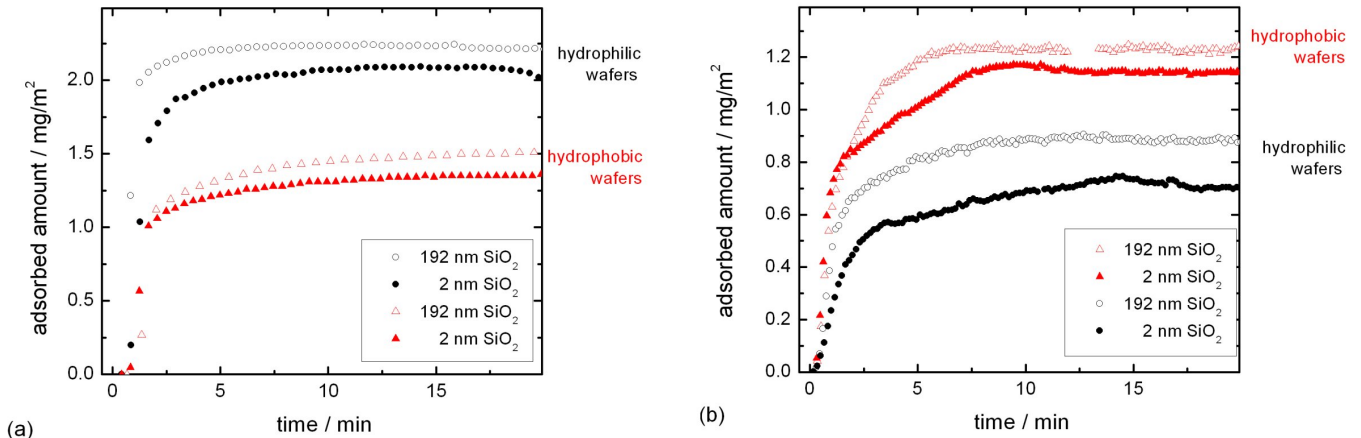


FIG. 2. Adsorption kinetics of (a) lysozyme and (b) amylase on the four different types of surfaces.

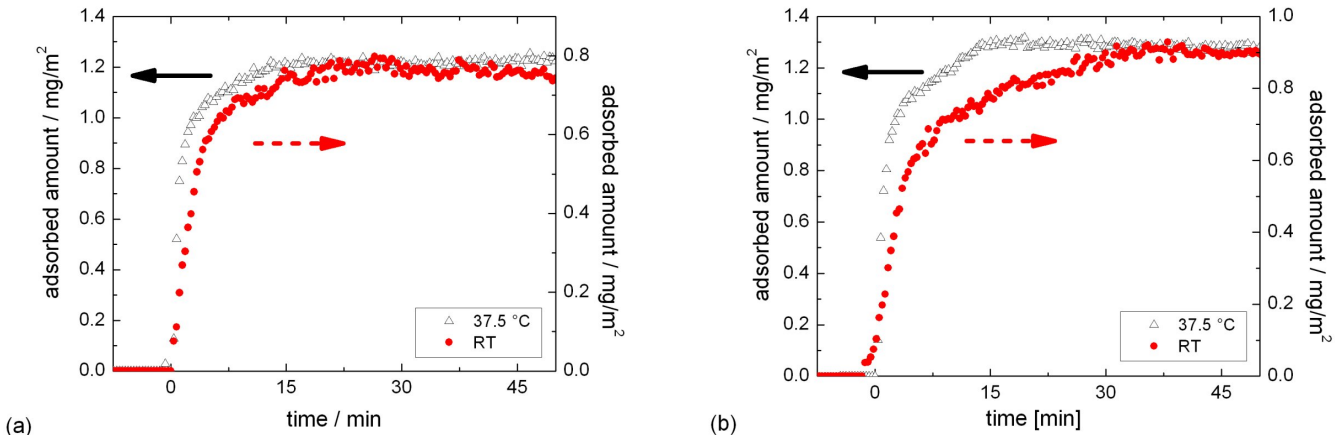


FIG. 3. BSA adsorption kinetics on hydrophobized silicon wafers with (a) thick and (b) thin oxide layers. Measurements at room temperature (RT) and 37.5°C are shown. A regime of constant adsorption rate can only be observed on wafers with thin oxide layers and the intermediate linear regime is elongated at room temperature.

III. MONTE CARLO APPROACH

The numerical investigation of biofilm adsorption is a challenging task since the number of degrees of freedom is huge if the detailed structure of the proteins is taken into account. In addition to this, proteins undergo structural changes at the surfaces which implies that the relaxation time for the adsorption of a single protein at the surface is out of scope for present simulation approaches. Therefore, a drastic reduction of the degrees of freedom is mandatory in order to simulate the adsorption of a protein film. In this section, we will briefly discuss the scope of different numerical approaches to protein dynamics.

The most fundamental methods are based on explicit quantum mechanical calculations. Incorporating the distribution of electrons they are able to predict

the forming of atomic bonds, which is indispensable for studying chemical reactions of proteins (see ref.[46] for an overview). Ab initio methods approximately solve Schrödinger's equation. Being able to provide very accurate results the calculations are very time consuming. To date, only a two-digit number of atoms can be simulated using this ab initio approach[47, 48]. Therefore, procedures have been developed[49–53] simplifying the unessential parts of the system using a semiempirical approach while describing the important parts using quantum mechanical methods. In these cases, the solvent is partly implicit.

Much larger systems can be considered by using fragment methods. Retaining the accuracy[54], these divide the whole system into several subunits which can be processed individually enabling the use of parallel comput-

ers. Differing in the underlying method, several fragment methods are known, e.g. FMO (fragment molecular orbital) method [55, 56], SFM (systematic fragmentation method) [57–59] and EFP (effective fragment potential) method [60, 61]. Fragmentation methods have the advantage that they are nearly fully quantum mechanical in nature, with classical approximations often used for long-range interactions. They can be used for the simulation of small proteins: Ishida analyzed [62] the role of a polar protein environment in a special enzymatic process using FMO. Ishikawa et al determined [63] the molecular interactions between the prion protein and GN8 (a potential curative agent for prion diseases) based on the fragment molecular orbital method, too. Due to the limitation of the system size and time scale, however, they can't be used in order to study protein adsorption involving conformational changes.

To overcome those limitations, quantum effects are often neglected. This is also the case for so-called full atomistic molecular dynamic simulations, where atoms are the smallest building blocks. By using these classical approaches, the simulation of peptides and small proteins becomes feasible. This includes forecasts of structural changes of single proteins and forecasts of possible transition paths between two states [64, 65]. It also includes the simulation of changes of conformation, such as simpler ones that involve only loop motions. Those take place on a nanosecond time scale, while large changes that involve the rearrangement of domains may occur on the microsecond to millisecond time scale [66]. These larger changes are still not accessible using an atomistic level of detail.

The time evolution of a system can be obtained via Molecular Dynamics, Brownian Dynamics or local Monte Carlo simulations, but the latter two have a limited ability of simulating the solvent, as they can only do it implicitly. Often this is done in MD, too, as means of speeding up a simulation, retaining the atomistic precision of the protein model. Whether this is reasonable for incidents like protein folding or adsorption is an open question [67]. Some results suggest that it is good enough [68], at least for folding. Another comparison of the influence of the level of detail of the solvent on the adsorption of peptides on hydrophobic surfaces is done by Sun and coworkers [69, 70] who find, that implicit solvent models yield very different results as compared to the explicit solvent model which was used as a reference. Also the different implicit solvent models predict different binding energies with varying level of agreement [69].

Further simplification for speeding up the simulations is done by combining multiple atoms to a single pseudo atom. This coarsened system needs to be described using modified force fields or interaction energies, respectively. For a fixed system size, the accessible time scales are two to three orders of magnitude higher than for a full all-atom description [71], so in principle they allow the simulation of large proteins. So far, however, the currently available generic force fields don't support struc-

tural changes in the tertiary structure [71]. Therefore, reliable simulations can be obtained *only* if the structure of the protein is maintained. An overview of those so called united atom or coarse-graining methods is given in ref. [72, 73].

Classical MD methods are based on the integration of Newton's equations. The numerical effort is very high, typical time scales are from 10 ns [74] up to some 10 μ s [67, 68], depending on the system size, the hardware being used and accuracy (ex- or implicit water) of the calculations. Raffaini et al for example were able to carry out simulations of the adsorption of single protein domains with α - [75] and β -sheets [76]. Later on they analyzed [77] the successive adsorption of protein fragments. The adsorption of a complete but small protein, lysozyme, including its conformational changes was simulated by Kubiak and Mulheran [78]. Details of the large scale MD simulations can be found in ref. [79].

Omitting the time evolution completely, greatly simplifying the solvent and the intermolecular interactions to the point of completely stiff proteins, interaction energies used to be calculated since two decades [80]. There are more recent publications using this approach [81, 82] proposing docking paths and preferred orientations, but conformational changes cannot be predicted by this procedure.

The range of applications for full atomistic as well as coarse-grained MD simulations indicate that these approaches cannot be used in order to simulate the adsorption of a full biofilm.

Speeding up the simulations by describing the interaction with the solvent molecules stochastically using the Langevin-equation results in a Brownian Dynamics simulation. Random forces with zero mean value mimic collisions of solvent molecules with the beads of a protein. Ravichandran et al [83] were able to show the possibility of adsorption of proteins with a positive net charge to a positively charged surfaces due to inhomogeneous charge distribution. Since then, however, the number of publications using Brownian Dynamics at atomistic level of detail is declined in favor of Molecular Dynamics.

Monte Carlo simulations provide another stochastic ansatz. They can be used both for time evolution of a system (when using local moves solely and detailed balance to reach a stationary state) or transition paths between two states. Simulations of coarse-grained lattice proteins were published some time ago: Anderson et al [84] studied the adsorption of a model protein to an oil/water interface and Castells and coworkers [85] analyzed surface induced conformational changes. Being more widespread and potentially more accurate, today's researchers tend to prefer the usage of MD simulations as a workhorse when generating the time evolution at atomistic level. Nevertheless, due to their flexibility, Monte Carlo simulations offer an alternative method: Knowing an initial and a final state of a protein, it is efficiently possible to sample the transition path between those two states [64, 86, 87]. Sadly, the position of atoms in a protein/surface complex

can't be extracted experimentally[3, 88]. Not knowing the adsorbed state beforehand, this method cannot be used for protein adsorption.

A more detailed review of the methods used for the simulation of conformational changes can be found in ref.[89].

A. Colloidal approaches

Coarsening the system under consideration even more, colloidal length scales of a few nm are reached. This results in a *substantial* increase of both spacial and temporal time scale, the latter up to the order of seconds to hours, depending on the level of complexity. In this context, the solvent is only implicitly taken into account and proteins typically are modelled as particles of high symmetry, e.g. spheres, allowing many thousands of proteins to be considered. The downside is the neglect of all their structural details including the distribution of charges and other details of the interactions which are relevant for very short distances. Yet, this is a necessary compromise in order to reach time scales that are experimentally relevant for the adsorption of a protein-biofilm.

A simple but very efficient approach to protein adsorption is the so-called Random Sequential Adsorption (RSA), which typically is a 2D model describing the parking problem omitting the particle's trajectory to the surface. In the simplest case, at every time step a particle tries to adsorb irreversibly to a random site by chance. The probability is determined using the Metropolis-Hastings algorithm in conjunction with a hard core potential. So the surface coverage only depends on the volume exclusion. The jamming coverage of this problem is described by Hinrichsen et al[90] and the maximum theoretical coverage by Toth[91]. There are several enhancements made to this simple model. The adsorption and desorption of particles in combination with a non-spherical geometry and a change of conformation was considered by van Tassel et al[92]. Also more complex potentials [93–95], e.g. for soft-RSA[96, 97] are taken into consideration. Furthermore, the effects of quasi-3D models using convex particles were studied by van Tassel and coworkers[92, 98]. Lavallo et al[99] analyzed an RSA variant, in which adsorbed particles are immobilized not before a certain amount of time, allowing them to find a more suitable spot minimizing the free energy of the adsorbed particles. Finally, there is a more recent attempt to model the reversible adsorption of binary mixtures[100] resulting in a simple formula for the prediction of steady state coverage of mixtures depending on the steady state coverage of the pure components. In any case, however, the comparison to experiments is limited, as fewer experimental parameters are realizable and the particle's trajectory to the surface is not accounted for.

On the colloidal level, often Brownian Dynamics simulations are used. In this case, interactions are typically within the DLVO framework[101–103] including

Coulomb interactions in a double layer, van der Waals interactions and additionally steric repulsion. Those publications analyze adsorption phenomena in general, in the latter, the parameters were chosen to mimic the adsorption of small globular proteins such as lysozyme. Spontaneous ordering depending on the ionic strength of the solvent is observed, too[101, 104].

B. Simulation of a biofilm using colloidal models with internal degrees of freedom

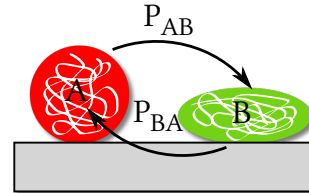


FIG. 4. Being adsorbed to a surface, particles may change their conformation by chance from a compact to an expanded state and vice versa using probabilities given by the Metropolis-Hastings algorithm.

Using local Monte Carlo simulations, it is easily possible to include internal degrees of freedom into the model. We use such an internal degree of freedom to model a reversible change of conformation of a protein from a compact to an expanded state on adsorption to the surface as shown in Fig. 4. The expanded state optimizes the surface interaction at the expense of the particle/particle interaction whereas the compact state minimizes the covered surface. Using this particle model we observe [8, 9] a considerable deviation from simple, Langmuir-like adsorption kinetics (cf. Fig. 5).

In this specific model, DLVO interactions were utilized and adjusted using experimentally known parameters to mimic amylase adsorbing to silicon wafers. However, due to the simplicity of the protein model many results are at least on qualitative level valid for other types of proteins as well.

The size of the simulation box is tiny compared to the volume of the experimental fluid cell. Applying a canonical ensemble for the whole simulation box, the drift of the protein concentration in the solvent would be largely overestimated. Therefore it was necessary to use two sub-volumes (cf. Fig. 6). The upper part was to mimic an infinite reservoir of particles using a grand canonical ensemble, whereas the lower part being in contact with the surface had to be simulated using a constant number of particles, which was only changed by particles entering or leaving the box by means of diffusion.

Particles adsorbing to the surface are directed to their adsorption site by the interaction with other particles already adsorbed. This is a major difference compared to RSA, where possible adsorption sites are chosen by

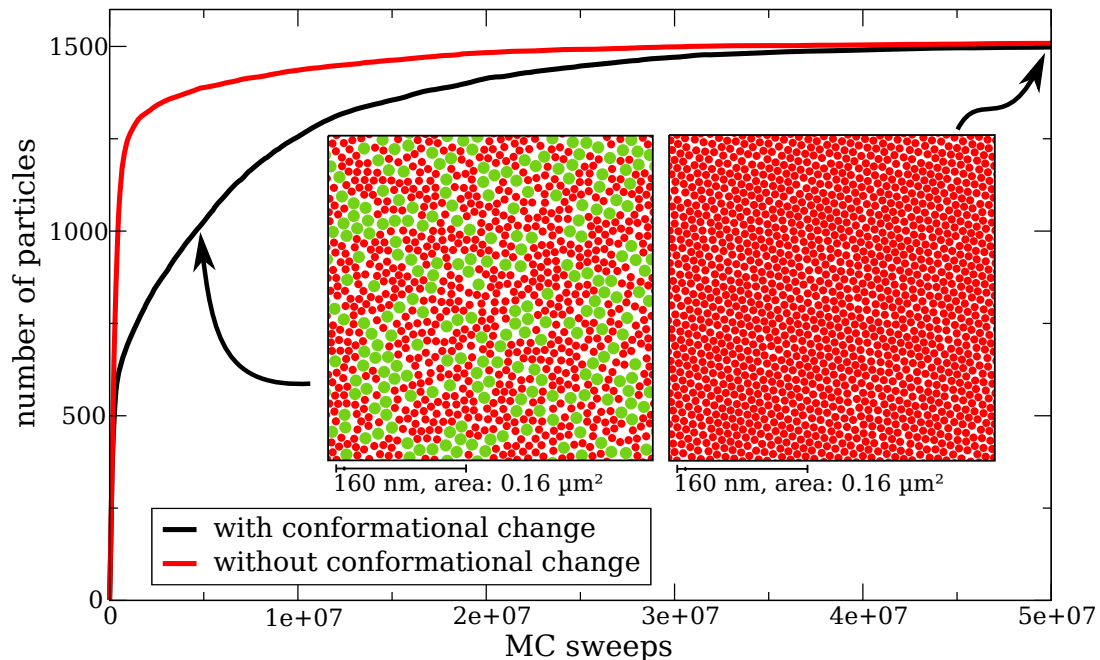


FIG. 5. The adsorption kinetics of simulations with (black) and without (red) change of conformation. For lower surface coverages, the expanded state is more stable than the compact one. Packing more particles to the surface, the contrary occurs.

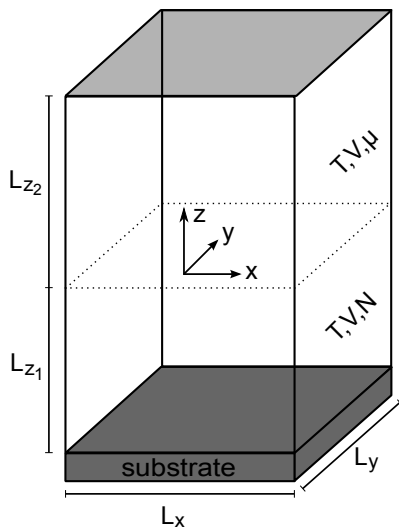


FIG. 6. Simulation box

chance. Fig. 7 shows two snapshots of the energy landscape a particle moves in when approaching the surface. In the second plot, there is enough free space, so that a particle can adsorb to the surface. As a consequence, the energy barrier evoked by the particles already adsorbed is lower than in the first plot. Passing this barrier, a particle is trapped in an attractive potential, as illustrated in Fig. 8. Therefore it has to following the iso line of the minimum and thus, the particle is directed to the adsorption site. Actually Fig.7 b) evolved from 7 a): Adsorbing to the surface, a particle moved it's neighbours a bit, so

that it could fit to the adsorption site. The particle was removed again for the plot to ensure a better comparison of the energy landscape. Typically the comparison with the experiment is achieved via the measured kinetics. It is suggested by experimental results that the deviation from Langmuir kinetics is due to long-ranged interactions with the silicon substrate below the oxide layer. Additionally, simulations indicate a similar deviation caused by conformational changes which are induced by long-ranged van der Waals interactions. So, combining experimental and theoretical results, we suppose that those van der Waals-induced conformational changes are the cause for the experimentally observed kinetics. Yet, as the same theoretical curves could possibly be generated in different ways, comparing the distribution of the adsorbed particles in both simulation and experiment would be desirable. Using ellipsometry, their positions are not available. Therefore, statistical properties like the pair correlation or Euler characteristics cannot be extracted from these experimental measurements. To overcome this deficiency *in situ* AFM measurements can be performed, as presented in the next section.

IV. IN SITU AFM IMAGING

Atomic force microscopy (AFM) was used to image the surface topography of the substrate as well as the adsorbed proteins *in situ*. For the first experiments, mica was used as substrate due to its simple handling and its smooth surface. The measurements were performed in TappingModeTM to minimize the influence of the scan-

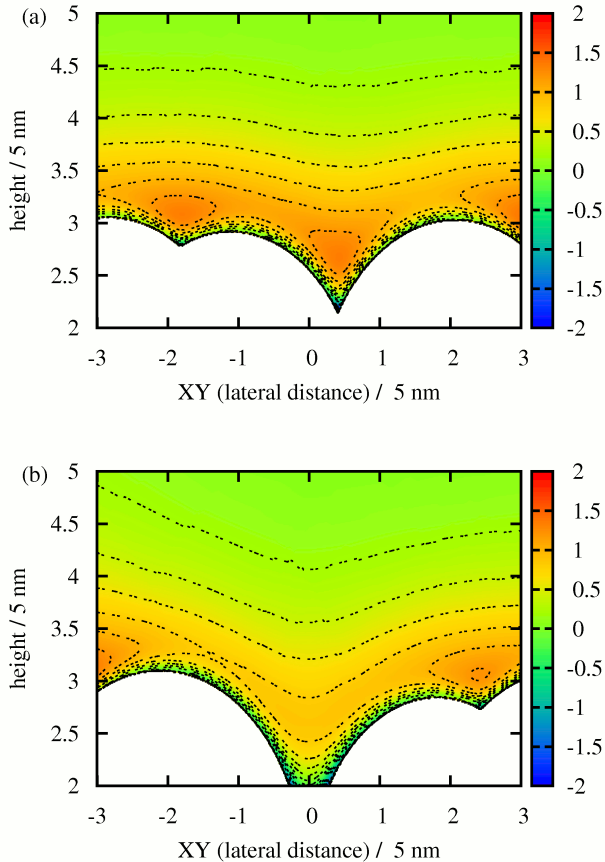


FIG. 7. The energy landscape of a particle approaching the surface for two different points in time. The isolines mark 0.2 steps, the white area has infinite potential energy.

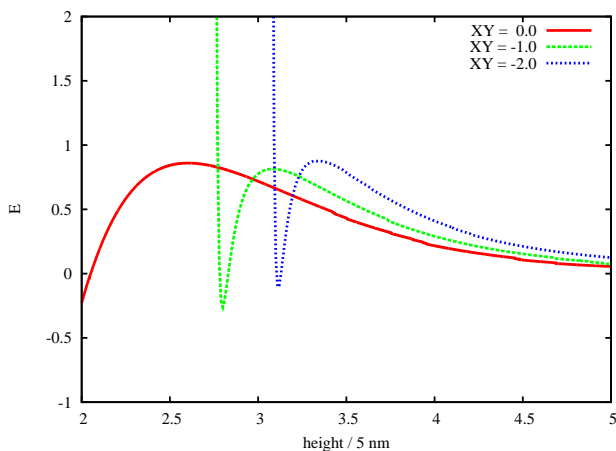


FIG. 8. The energy landscape of a particle approaching the surface. This is a plot of the potential energy for different lateral distances as shown in Fig. 7 b).

ning tip on the proteins. A triangular cantilever (OTR 8 or SNL, Veeco, Santa Barbara) was oscillated at a frequency of about 9 kHz. The scanning rate was between 0.5 to 1.5 scan lines per second depending on the scanning size (ranging from $(0.5 \mu\text{m})^2$ to $(3 \mu\text{m})^2$). The lateral resolution of the scans was either 256 or 512 pixels per line. The measurements were carried out in a closed fluid cell (Model MTFML, TappingModeTMFluid Cell, Veeco, Santa Barbara) using a MultiMode (Nanoscope III, Veeco, Santa Barbara). The cell was connected to a flow system (same set-up as in ellipsometry measurements) to allow for the exchange of buffer and protein solution. Experiments were performed at room temperature. Mica being frequently used for protein adsorption studies via AFM [33–38] was chosen as a substrate.

The mica was mounted in the fluid cell directly after cleavage and consequently exposed to acetate buffer of pH 4.75 at a concentration of 10 mM and ionic strength of 8 mM. A control scan of the mica surface was taken before exposing the surface to protein solution. At intervals of 5 to 10 minutes, the flow was stopped and topographic scans of the surface were taken (see Fig. 10). To ensure the absence of scan artifacts, as often reported [105–108], the scan area was enlarged several times to check for possible scan damage due to the tip. Under the experimental conditions mentioned above (pH, ionic strength), no influence of scanning on the distribution of the adsorbed proteins was observed. However, increasing the ionic strength of the solution lead to significant disturbance of the protein pattern upon scanning.

By *in situ* scanning, we avoid artifacts arising from the use of linker molecules like glutaraldehyde which typically lead to network-like structures (see Fig. 9(c)) or drying. Both procedures are frequently used in most AFM studies on protein adsorption to enable scanning in air [9, 35, 37, 38, 109].

The single objects imaged on the mica can be assigned to single proteins by their dimensions. The bright objects in Fig. 10 have an ellipsoidal shape with a long axis of 22 ± 7 nm and a short axis of 15 ± 5 nm (without tip deconvolution: nominal tip radius 15 nm). These dimensions are in good agreement with the dimensions reported in the literature [2] ($14 \times 4 \times 4$ nm³) indicating that single BSA molecules are displayed on the surface. The height of the proteins ranges between 0.7 and 1.6 nm depending on the scanning parameters in TappingModeTM AFM. Therefore it is not a reliable measure for such small and soft objects.

For the measurements on mica, no surface mobility was detected. The interaction between the negatively charged mica and the BSA is believed to hinder the mobility of the proteins. This attractive forces could be screened by solutions of higher ionic strength. However, reducing the attraction between the proteins and the surface leads to fragile scanning conditions, as mentioned above.

The proteins were not found to preferentially form clusters on the surface but rather form a random distribution [110]. To objectively characterize the distri-

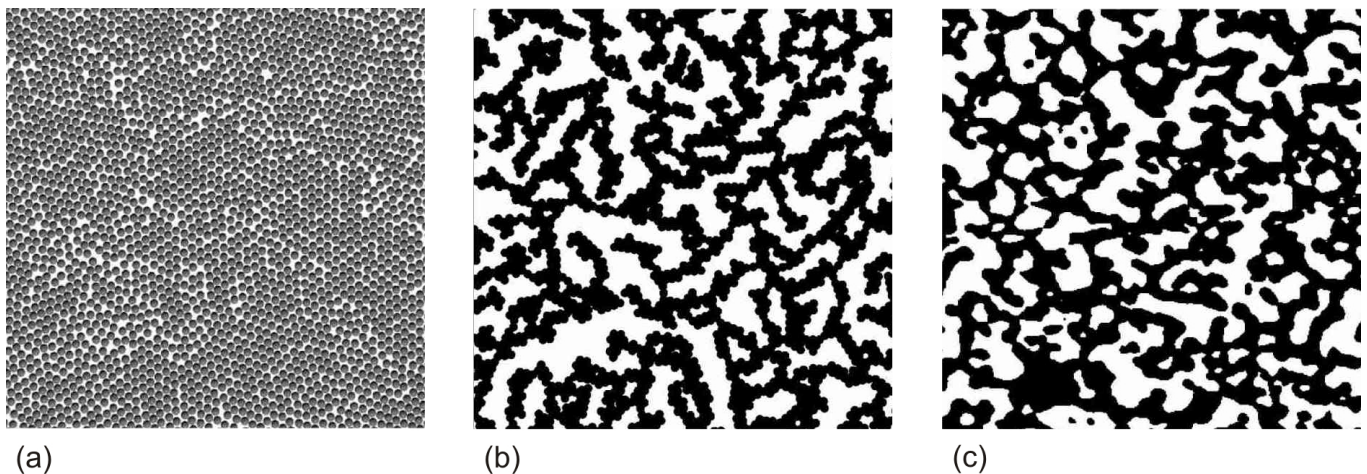


FIG. 9. The effect of linker molecules for a stabilization of a protein film: (a) Initial configuration in the MC simulations using the standard form of interactions. (b) Stationary configuration in the computer simulation after adding a short ranged contribution to the particle-particle interactions to mimic the effect of a linker. (c) Experimental view of an amylase film stabilized by glutaraldehyde. For a simple comparison with the simulations, a threshold has been applied to the high scale such that protein is black and substrate is white.

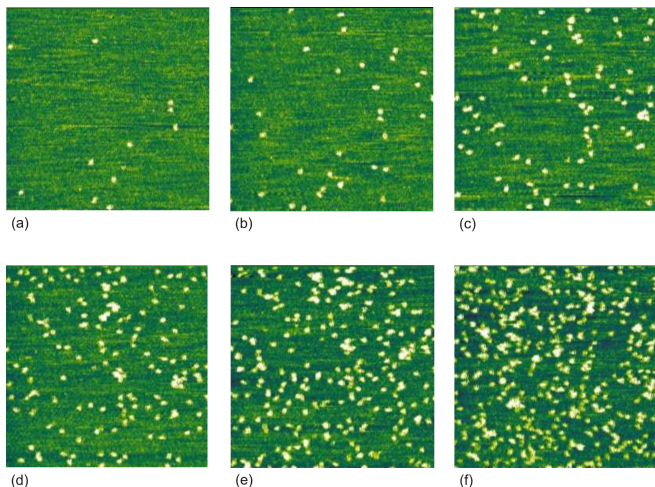


FIG. 10. Series of consecutive AFM images ($1\mu\text{m} \times 2\mu\text{m}$) of BSA ($20\mu\text{l}$ of 0.1mM protein solution in acetate buffer of pH 4.75 and ionic strength $I=8\text{mM}$ at room temperature) adsorbed onto mica taken at the same area (slight drift) under stopped flow conditions. The bright objects represent single proteins.

bution of these proteins on the surface, a two dimensional Minkowski analysis will be used. The Minkowski measures (in two dimensions: covered area, boundary length and Euler characteristics) are quantities that integrate over all n-point correlation functions. This leads to an excellent signal to noise ratio and allows for the structural analysis also for a small number of samples. The Minkowski analysis has successfully been applied to characterize point patterns in biology [111], astronomy [112] and dewetting processes [113]. The knowledge of the statistics of adsorption sites will open an opportu-

nity to determine the interaction potential between the adsorbed proteins and their surface mobility by comparison of experimental results and simulations.

V. SUMMARY AND CONCLUSIONS

The experimental and theoretical characterization of protein biofilms is a challenging task. In this work we used a number of different methods in order to characterize the adsorption kinetics of proteins at different kinds of surfaces. The experimental results showed that both the long- and the short-ranged interactions influence strongly the adsorption kinetics of the proteins. By means of ellipsometry, it has been shown that flexible proteins as e.g. amylase and BSA show an intermediate linear regime upon adsorption on Si wafers with thin oxide layer. Complementary computer simulations, which describe the proteins as single spherical particles with an internal degree of freedom indicate that this kind of kinetics is the result of conformational changes induced by density-density fluctuations. This scenario has been tested experimentally by using different kinds of proteins and substrates. Yet the adsorption of more rigid proteins – like lysozyme – led to a Langmuir-like adsorption kinetics on all Si wafer types.

A future challenge is to *in situ* study the adsorption site statistics as the surface coverage increases, which enables a direct comparison of experimental and theoretical results. A proof-of-concept is given by *in situ* AFM scans of BSA on mica. Future experiments will explore regimes of different surface mobility of the adsorbing molecules.

To sum up, three points are important for future biofilm studies: i) Van der Waals forces must be taken into account (therefore a detailed characterization of

samples is mandatory), ii) conformational changes upon adsorption can be triggered by particle-particle and by particle-surface interactions (where long-ranged forces have to be taken into account, too) and iii) colloidal sim-

ulations are currently the only method of choice for describing the kinetics of these systems, which spans over minutes to hours.

-
- [1] W. Norde, *Advances in Colloids and Interface Science* **25**, 267 (1986).
- [2] *Biopolymers at Interfaces*, edited by M. Malmsten (Marcel Dekker, Inc., 2003).
- [3] J. J. Gray, *Current Opinion in Structural Biology* **14**, 110 (Feb. 2004), ISSN 0959-440X.
- [4] F. A. Denis, P. Hanarp, D. S. Sutherland, J. Gold, C. Mustin, P. Rouxhet, and Y. F. Dufrêne, *Langmuir* **18**, 819 (2002).
- [5] K. E. Michael, V. N. Vernekar, B. G. Keselowsky, J. Meredith, R. A. Latour, and A. J. Garcia, *Langmuir* **19**, 8033 (2003).
- [6] *Integrin binding specificity regulates biomaterial surface chemistry effects on cell differentiation*, Vol. 102.
- [7] W. Teughels, N. V. Assche, I. Sliepen, and M. Quirynen, *Clinical Oral Implants Research* **17**, 68 (2006).
- [8] A. Quinn, H. Mantz, M. Bellion, and K. Jacobs, *Europhysics Letters* **81**, 56003 (2008).
- [9] M. Bellion, L. Santen, H. Mantz, H. Hähl, A. Quinn, A. Nagel, C. Gilow, C. Weitenberg, Y. Schmitt, and K. Jacobs, *Journal of Physics: Condensed Matter* **20**, 404226 (2008).
- [10] R. Seemann, S. Herminghaus, and K. Jacobs, *Journal of Physics: Condensed Matter* **13**, 4925 (2001).
- [11] R. Seemann, S. Herminghaus, and K. Jacobs, *Physical Review Letters* **86**, 5524 (2001).
- [12] R. Seemann, S. Herminghaus, C. Neto, S. Schlagowski, D. Podzimek, R. Konrad, H. Mantz, and K. Jacobs, *Journal of Physics: Condensed Matter* **17**, 5267 (2005).
- [13] G. Huber, S. Herminghaus, R. Spolenak, K. Mecke, K. Jacobs, N. S. Gorb, and E. Arzt, *Proceedings of the National Academy of Sciences* **102**, 16293 (2005).
- [14] J. Israelachvili, *Intermolecular & Surface Forces*: (Academic Press Inc., 1992).
- [15] C. F. Schmidt, R. M. Zimmermann, and H. E. Gaub, *Biophysical Journal* **57**, 577 (1990).
- [16] C. F. Wertz and M. M. Santore, *Langmuir* **18**, 1190 (2002).
- [17] R. Ishiguro, Y. Yokoyama, H. Maeda, A. Shimamura, K. Kemeyama, and K. Hiramatsu, *Journal of Colloids and Interface Science* **290**, 91 (2005).
- [18] S. Daly, T. M. Przybycien, and R. D. Tilton, *Langmuir* **19**, 3848 (2003).
- [19] L. Baujard-Lamotte, S. Noinville, F. Boubard, P. Marque, and E. Pauthe, *Colloids and Surfaces B: Biointerfaces* **63**, 129 (2008).
- [20] W. Norde and J. P. Favier, *Colloids and Surfaces* **64**, 87 (1992).
- [21] J. Foster, "Albumin structure, function and uses," (Oxford; New York; Pergamon Press, 1977) pp. 53–84.
- [22] D. C. Carter and J. X. Ho, "Advances in protein chemistry," (Academic Press, 1994) Chap. Structure of Serum Albumin, pp. 153 – 203.
- [23] J. R. Olivieri and A. F. Craievich, *European Biophysics Journal* **24**, 77 (1995).
- [24] K. Hirayama, S. Akashi, M. Furuya, and K. ichi Fukuhara, *BIOCHEMICAL AND BIOPHYSICAL RESEARCH COMMUNICATIONS* **173**, 639 (1990).
- [25] S. Hu, M. Y. Xie, P. Ramachandran, R. R. O.Loo, J. A. Loo, and D. T. Wong, *Proteomics* **5**, 1714 (2005).
- [26] T. Arnebrant, "Biopolymers at interfaces," (Marcel Dekker, Inc., 2003) Chap. Protein Adsorption in the Oral Environment, pp. 811–855.
- [27] C. M. Roth and A. M. Lenhoff, *Langmuir* **11**, 3500 (1995).
- [28] D. Malamud and J. W. Drysdale, *Analytical Biochemistry* **86**, 620 (1978).
- [29] S. R. Wasserman, G. M. Whiteside, I. M. Tidswell, B. M. Ocko, P. S. Pershan, and J. D. Axe, *Journal of the American Chemical Society* **111**, 5852 (1989).
- [30] J. B. Brzoska, I. B. Azouz, and F. Rondelez, *Langmuir* **10**, 4367 (1994).
- [31] T. A. Mykhaylyk, S. D. Evans, C. Fernyhough, I. Hamley, and J. R. Henderson, *Journal of Colloid and Interface Science* **260**, 234 (2003).
- [32] R. Zimmermann, S. Dukhin, and C. Werner, *Journal of the Physical Chemistry B* **105**, 8544 (2001).
- [33] D. T. Kim, H. W. Blach, and C. J. Radke, *Langmuir* **18**, 5841 (2002).
- [34] L. P. Silva, *Current Protein and Peptide Science* **v6**, 387 (2005).
- [35] J. W. C. Cheung and G. C. Walker, *Langmuir* **24**, 13842 (2008).
- [36] O. Ouerghi, A. Touhami, A. Othmane, H. B. Ouada, C. Martelet, C. Fretigny, and N. Jaffrezic-Renault, *Biomeolecular Engineering* **19**, 183 (2002).
- [37] M. Bergkvist, J. Carlsson, T. Karlsson, and S. Oscarsson, *Journal of Colloid and Interface Science* **206**, 475 (1998).
- [38] K. L. Marchin and C. L. Berrie, *Langmuir* **19**, 9883 (2003).
- [39] P. A. Cuyper, J. W. Corsel, M. P. Janssen, J. M. Kop, W. T. Hermens, and H. C. Hemker, *Journal of Biological Chemistry* **258**, 2426 (1983).
- [40] J. Vörös, *Biophysical Journal* **87**, 553 (2004).
- [41] R. M. A. Azzam and N. M. Bashara, *Ellipsometry and Polarized Light* (North Holland, 1977).
- [42] J. A. de Feijter, J. Benjamins, and F. A. Veer, *Biopolymers* **17**, 1759 (1978).
- [43] V. Ball and J. J. Ramsden, *Biopolymers* **46**, 489 (1998).
- [44] C. Tanford, *Science* **200**, 1012 (1978).
- [45] Being precise, not only oxide layer thickness shall be characterized, also the refractive index, since depending on the production process, different porosities of amorphous Si dioxide layers can be gained.
- [46] D. Marx, *ChemPhysChem* **7**, 1848 (2006).
- [47] R. A. Latour, *Biointerphases* **3**, FC2 (2008).
- [48] A. Rimola, M. Corno, C. M. Zicovich-Wilson, and P. Ugliengo, *Physical Chemistry Chemical Physics* **11**, 9005 (2009).

- [49] E. Nikitina, V. Sulimov, F. Grigoriev, O. Kondakova, and S. Lushechina, *International Journal of Quantum Chemistry* **106**, 1943 (2006).
- [50] E. Nikitina, V. Sulimov, V. Zayets, and N. Zaitseva, *International Journal of Quantum Chemistry* **97**, 747 (2004).
- [51] M. Wada and M. Sakurai, *Journal of Computational Chemistry* **26**, 160 (2005).
- [52] N. Yu, H. P. Yennawar, and K. M. M. Jr, *Acta Crystallographica Section D Biological Crystallography* **61**, 322 (2005), ISSN 0907-4449.
- [53] R. A. Friesner and V. Guallar, *Annual Review of Physical Chemistry* **56**, 389 (May 2005), ISSN 0066426X.
- [54] M. S. Gordon, J. M. Mullin, S. R. Pruitt, L. B. Roskop, L. V. Slipchenko, and J. A. Boatz, *The Journal of Physical Chemistry B* **113**, 9646 (Jul. 2009).
- [55] D. G. Fedorov and K. Kitaura, *The Journal of Physical Chemistry A* **111**, 6904 (2007).
- [56] H. Li, D. G. Fedorov, T. Nagata, K. Kitaura, J. H. Jensen, and M. S. Gordon, *Journal of Computational Chemistry* **31**, 778 (2010).
- [57] V. Deev and M. A. Collins, *The Journal of Chemical Physics* **122**, 154102 (Apr. 2005).
- [58] M. A. Collins and V. A. Deev, *The Journal of Chemical Physics* **125**, 104104 (2006).
- [59] M. A. Collins, *The Journal of Chemical Physics* **127**, 024104 (Jul. 2007).
- [60] M. S. Gordon, M. A. Freitag, P. Bandyopadhyay, J. H. Jensen, V. Kairys, and W. J. Stevens, *The Journal of Physical Chemistry A* **105**, 293 (2001).
- [61] R. M. Minikis, V. Kairys, and J. H. Jensen, *The Journal of Physical Chemistry A* **105**, 3829 (Apr. 2001).
- [62] T. Ishida, *The Journal of Chemical Physics* **129**, 125105 (2008), ISSN 00219606.
- [63] T. Ishikawa, T. Ishikura, and K. Kuwata, *Journal of Computational Chemistry* **30**, 2594 (2009), ISSN 01928651.
- [64] P. G. Bolhuis, D. Chandler, C. Dellago, and P. L. Geissler, *Annual Review of Physical Chemistry* **53**, 291 (2002), ISSN 0066-426X.
- [65] M. K. Kim, G. S. Chirikjian, and R. L. Jernigan, *Journal of Molecular Graphics and Modelling* **21**, 151 (Oct. 2002), ISSN 1093-3263.
- [66] D. Kern and E. R. P. Zuiderweg, *Current Opinion in Structural Biology* **13**, 748 (Dec. 2003), ISSN 0959-440X, PMID: 14675554.
- [67] P. L. Freddolino, F. Liu, M. Gruebele, and K. Schulten, *Biophysical Journal* **94**, L75 (May 2008), ISSN 0006-3495.
- [68] V. A. Voelz, G. R. Bowman, K. Beauchamp, and V. S. Pande, *Journal of the American Chemical Society* **132**, 1526 (Feb. 2010).
- [69] Y. Sun and R. A. Latour, *Journal of Computational Chemistry* **27**, 1908 (2006).
- [70] Y. Sun, B. N. Dominy, and R. A. Latour, *Journal of Computational Chemistry* **28**, 1883 (2007).
- [71] L. Monticelli, S. K. Kandasamy, X. Periole, R. G. Larson, D. P. Tieleman, and S. Marrink, *Journal of Chemical Theory and Computation* **4**, 819 (May 2008).
- [72] V. Tozzini, *Current Opinion in Structural Biology* **15**, 144 (Apr. 2005), ISSN 0959-440X.
- [73] T. Bereau and M. Deserno, *The Journal of Chemical Physics* **130**, 235106 (Jun. 2009).
- [74] M. Karplus and J. A. McCammon, *Nat Struct Mol Biol* **9**, 646 (2002), ISSN 1072-8368.
- [75] G. Raffaini and F. Ganazzoli, *Langmuir* **19**, 3403 (Apr. 2003).
- [76] G. Raffaini and F. Ganazzoli, *Langmuir* **20**, 3371 (Apr. 2004).
- [77] G. Raffaini and F. Ganazzoli, *Journal of Materials Science: Materials in Medicine* **18**, 309 (Feb. 2007).
- [78] K. Kubiak and P. A. Mulheran, *The Journal of Physical Chemistry B* **113**, 12189 (2009).
- [79] J. L. Klepeis, K. Lindorff-Larsen, R. O. Dror, and D. E. Shaw, *Current Opinion in Structural Biology* **19**, 120 (Apr. 2009), ISSN 0959-440X.
- [80] D. R. Lu and K. Park, *Journal of Biomaterials Science. Polymer Edition* **1**, 243 (1990), ISSN 0920-5063, PMID: 2279006.
- [81] C. J. Camacho and S. Vajda, *Proceedings of the National Academy of Sciences of the United States of America* **98**, 10636 (Sep. 2001), ISSN 0027-8424, PMID: 11517309 PMID: 58518.
- [82] H. Hsu, S. Sheu, and R. Tsay, *Colloids and Surfaces B: Biointerfaces* **67**, 183 (Dec. 2008), ISSN 0927-7765.
- [83] S. Ravichandran, J. D. Madura, and J. Talbot, *The Journal of Physical Chemistry B* **105**, 3610 (May 2001).
- [84] R. E. Anderson, V. S. Pande, and C. J. Radke, *The Journal of Chemical Physics* **112**, 9167 (May 2000).
- [85] V. Castells, S. Yang, and P. R. V. Tassel, *Physical Review E* **65**, 031912 (Mar. 2002).
- [86] Y. Q. Gao, L. Yang, Y. Fan, and Q. Shao, *International Reviews in Physical Chemistry* **27**, 201 (Apr. 2008), ISSN 0144235X.
- [87] F. A. Escobedo, E. E. Borrero, and J. C. Araque, *Journal of Physics: Condensed Matter* **21**, 333101 (2009), ISSN 0953-8984.
- [88] K. Makrodimitris, D. L. Masica, E. T. Kim, and J. J. Gray, *Journal of the American Chemical Society* **129**, 13713 (2007), ISSN 0002-7863.
- [89] A. van der Vaart, *Theoretical Chemistry Accounts: Theory, Computation, and Modeling (Theoretica Chimica Acta)* **116**, 183 (2006).
- [90] E. L. Hinrichsen, J. Feder, and T. Jøssang, *Journal of Statistical Physics* **44**, 793-827 (1986).
- [91] L. Toth, *Mathematica* **30**, 1-3 (1983), ISSN 0025-5793.
- [92] P. R. V. Tassel, P. Viot, and G. Tarjus, *The Journal of Chemical Physics* **106**, 761-770 (1997).
- [93] J. Talbot, G. Tarjus, P. R. V. Tassel, and P. Viot, *Colloids and Surfaces A: Physicochemical and Engineering Aspects* **165**, 287-324 (May 2000), ISSN 0927-7757.
- [94] Z. Adamczyk and P. Weronki, *Journal of Colloid and Interface Science* **189**, 348-360 (May 1997), ISSN 0021-9797.
- [95] M. R. Oberholzer, J. M. Stankovich, S. L. Carnie, D. Y. C. Chan, and A. M. Lenhoff, *Journal of Colloid and Interface Science* **194**, 138-153 (Oct. 1997), ISSN 0021-9797.
- [96] M. Semmler, E. K. Mann, J. Rička, and M. Borkovec, *Langmuir* **14**, 5127 (1998).
- [97] Z. Adamczyk, M. Zembala, B. Siwek, and P. Warszyński, *Journal of Colloid and Interface Science* **140**, 123 (Nov. 1990), ISSN 0021-9797.
- [98] P. R. V. Tassel, P. Viot, G. Tarjus, and J. Talbot, *The Journal of Chemical Physics* **101**, 7064-7073 (Oct. 1994).
- [99] P. Lavalle, P. Schaaf, and M. Ostafin, *Proc. Natl. Acad. Sci. USA* **96**, 11100 - 11105 (Sep. 1999).

- [100] I. Lončarević, L. Budinski-Petković, and S. B. Vrhovac, *Physical Review E* **76**, 031104 (2007).
- [101] M. Miyahara, S. Watanabe, Y. Gotoh, and K. Higashitani, *The Journal of Chemical Physics* **120**, 1524–1534 (2004).
- [102] S. Ravichandran, *Biophysical Journal* **78**, 110 (2000), ISSN 00063495.
- [103] M. R. Oberholzer, N. J. Wagner, and A. M. Lenhoff, *The Journal of Chemical Physics* **107**, 9157–9167 (Dec. 1997).
- [104] S. Watanabe, M. Miyahara, and K. Higashitani, *The Journal of Chemical Physics* **122**, 104704 (Mar. 2005).
- [105] A. S. Lea, A. Pungor, V. Hlady, J. D. Andrade, J. N. Herron, and J. E. W. Voss, *Langmuir* **8**, 68 (1992).
- [106] A. Agnihotri and C. A. Siedlecki, *Langmuir* **20**, 8846 (2004).
- [107] C. A. Siedlecki, S. J. Eppel, and R. E. Marchant, *Journal of Biomedical Materials Research* **28**, 971 (1994).
- [108] S. J. Eppell, F. R. Zypman, and R. E. Marchant, *Langmuir* **9**, 2281 (1993).
- [109] H. Agheli, J. Malmström, E. Larsson, M. Textor, and D. S. Sutherland, *Nanoletters* **6**, 1165 (2006).
- [110] Y. Schmitt, K. Mecke, K. Jacobs, O. Leidinger, and L. Santen, to be published.
- [111] K. R. Mecke and D. Stoyan, *Biometrical Journal* **1996**, 1 (2005).
- [112] K. R. Mecke, T. Buchert, and H. Wagner, *Astronomy and Astrophysics* **288**, 697 (1994).
- [113] S. Herminghaus, K. Jacobs, K. Mecke, J. Bischof, A. Fery, M. Ibn-Elhaj, and S. Schlagowski, *Science* **282**, 916 (1998).